Inhibition of step-flow crystal growth on the {110} face of α-HgI_2 by a high coverage factor

Oleg A. Louchev*
Research Center for Technological Lasers of Russian Academy of Sciences, Troitsk, Moscow District, 142092, Russia
(Received 22 January 1996; revised manuscript received 19 June 1996)

The problem of step-flow crystal growth is considered for the specific case of the {110} face of α-HgI_2. It is shown that the step-flow growth is inhibited by adsorption and high coverage factor ranging from 0.2 to 0.3. The time for full coverage of the adlayer is the same order of magnitude as the adsorption time, and influences therefore the characteristic time of the step-flow problem, relevant diffusion length, and step-flow velocity. Step-flow growth proceeds under kinetic/diffusion or diffusion control. The case of kinetic/diffusion control should reveal itself in the rectangular form of screw dislocation growth spirals with rounded sides and corners (the extent of corner rounding should correspond to characteristic diffusion length, $\cong 1-3$ μm), while the case of diffusion control should reveal itself in the circular form of dislocation spirals. Suggested values of the adsorption energy $E_a \cong (0.55-0.6)\Delta H \cong 0.63-0.69$ eV (with steric factor within the range of $S=1-0.3$, respectively) and activation energy of incorporation into steps $\cong 0.3-0.35$ eV give a good agreement of the growth rates obtained within the framework of the step-flow model considered with three different sets of experimental data [T. Kobayashi *et al.*, J. Electrochem. Soc. **130**, 1183 (1983); M. Isshiki *et al.*, J. Cryst. Growth **102**, 344 (1990); M. Zha *et al.*, *ibid.* **115**, 43 (1991)]. [S0163-1829(96)05847-X]

I. INTRODUCTION

The physics of step-flow crystal growth are of fundamental interest for understanding the background phenomena of microscale structures appearing in crystalline matter and as well as for a number of modern techniques of production of artificial crystals and films for different applications. Since the seminal work by Burton, Cabrera, and Frank,[1] a great number of papers have concentrated on mechanisms and different modes of step-flow growth.[2,3] The work by Bales and Zangwill[4] focused on the morphological instability of steps due to the different incorporation rates of atoms diffusing to the steps from upper and lower terraces.[5] This initiated a series of publications in this field which elucidates the role of various effects occurring in different modes of step-flow instability, leading to step meandering and the appearance of dendritic structures on growth interface.[6–10]

Current work focuses on the step-flow growth phenomena on the {110} face of α-HgI_2 occurring in physical vapor transport growth technique. Bulk crystals of α-HgI_2 grown by this technique are of interest as an effective detecting material of spectrometric quality with high yield,[11] suitable for a number of x- and γ-ray applications. The physical transport growth of this crystal has been extensively studied both experimentally[12–18] and theoretically.[19–23] Nevertheless, the growth kinetics of these crystals are not understood well. The experimental research has shown a strong inhibition of the growth rate with time.[13–15,17] This was later attributed to the conductive heat resistance of the growing crystal,[12] the interplay of conductive and radiation heat transfer,[19–22] also coupled together with mass transfer limitations.[23] The relevant theoretical models[19–23] have so far focused on the different mass transport and heat transport phenomena. These models consider the growth rate in the linear[23] and parabolic[20,23] approximations using the kinetic coefficients estimated from different growth experiments, and do not take into account the microscale kinetics of growth which may proceed via a screw dislocation with a flow of macrosteps.

The present paper focuses on a theoretical study of the step-flow growth kinetics on the {110} face with an account of relevant surface phenomena. It is shown that the step-flow growth on the {110} face is strongly inhibited by the adsorption and high coverage factor in the adlayer. The growth rates obtained in the framework of the step-flow model are compared with three different sets of experimental data. The paper is structured as follows. The step-flow model used in this study is given in Sec. II. In Sec. III, the main results are presented together with relevant discussion. The final conclusions are given in Sec. IV.

II. STEP-FLOW MODEL

Let us consider a simplified scheme of a crystal face in the form of a sequence of macrosteps, with a given interstep distance λ and height H. The crystal is supposed to grow from the vapor under a partial pressure P_0 corresponding to the source of the material held at the temperature T_0, i.e., $P_0=P_e(T_0)$, where $P_e(T)$ is the equilibrium pressure/temperature equation.[24] In this study, we will neglect the gas-phase-diffusion limitation of the process assuming that the growth is controlled by interface kinetics, so that the gas pressure in front of the growth interface corresponds to the pressure in the source zone, P_0. We neglect also the contribution from the direct collisions into steps, taking into account only surface diffusion.

The problem is considered within the framework of the Burton, Cabrera, and Frank (BCF) model, taking into account the following sequence of events: (i) physical adsorption/desorption, (ii) diffusion transport of adsorbed molecules over the terraces to the steps, and (iii) thermally activated incorporation of molecules arriving at steps from corresponding upper and lower terraces. Let us consider one isolated terrace in the reference frame of the moving step. The surface distribution of molecules adsorbed on the terrace, n, is governed by

$$D(T_i)\frac{d^2n}{dx^2}+\frac{P_0}{(2\pi mk_BT_i)^{1/2}}\left(1-\frac{n}{n_a}\right)S\ \exp\left(-\frac{\delta E_a}{k_BT_i}\right)$$
$$-n\nu\ \exp\left(-\frac{E_a+\delta E_a}{k_BT_i}\right)=0. \quad (1)$$

Here $n(x)$ is the surface density of adsorbed molecules, T_i is the temperature on the terrace, k_B is the Boltzmann constant, $\nu\approx10^{13}$ Hz is the thermal vibration frequency, E_a is the adsorption energy, $n_e(T)$ is the equilibrium density of adsorbed molecules, $D(T_i)=n_a{}^{-1}\nu\ \exp(-E_d/k_BT_i)$ is the surface diffusion coefficient, n_a is the density of the adsorption sites, m is the molecular mass, E_d is the energy of activation of surface diffusion. The factor $(1-n/n_a)S\ \exp(-\delta E_a/k_BT_i)$ in the adsorption term of Eq. (1) represents the probability of adsorption, taking into account the fraction of free adsorption sites on the terrace $(1-n/n_a)$ and condensation coefficient equated to a steric factor S,[25] times the probability of overcoming an activation energy of adsorption δE_a.

In addition, the so-called radiation boundary condition[9] is used at the step:

$$x=0,\quad D(T_i)\frac{dn}{dx}=\beta(T_i)\{n-n_e(T_i)\}. \quad (2)$$

The symmetry of the problem gives

$$x=\lambda/2,\quad \frac{dn}{dx}=0. \quad (3)$$

The kinetic coefficient (or attachment rate constant), $\beta(T_i)$, is the Arrhenius-type constant given by

$$\beta(T_i)\cong\frac{a_0^2}{\lambda_k}\nu\ \exp(-\delta E_{\rm inc}/k_BT_i), \quad (4)$$

where λ_k is the mean distance between the kinks on the step, a_0 is the intermolecular distance on the step, and $\delta E_{\rm inc}$ is the activation energy of the molecule incorporation into the step. It should be noted here that this energy barrier may differ for the two terraces adjacent to the step with the preferential attachment from the lower one.[5] However, this effect is neglected here.

The velocity of the step-flow growth is given by

$$V=\frac{2h}{H}s_0\beta(T_i)\{n(0)-n_e(T_i)\}, \quad (5)$$

where h is the height of monolayer, s_0 is the characteristic area per one molecule, and H is the height of the step (which may include several layers).

The solution to Eqs. (1)–(5) gives the following expression for the step-flow velocity:

$$V=\frac{h}{H}\frac{2s_0D(T_i)}{\lambda_D}\frac{\tanh(\lambda/2\lambda_D)}{1+\dfrac{\tanh(\lambda/2\lambda_D)D}{\beta\lambda_D}}$$
$$\times\tau^*S\ \exp\left(-\frac{\delta E_a}{k_BT_i}\right)\frac{P_0-P_e(T_i)}{(2\pi mk_BT_i)^{1/2}}, \quad (6)$$

where $\lambda_D=(D\tau^*)^{1/2}$ is the diffusion length,

$$\tau^*=\frac{\tau_1\tau_2}{\tau_1+\tau_2}, \quad (7)$$

is the characteristic time with

$$\tau_1=\nu^{-1}\exp[(E_a+\delta E_a)/k_BT_i], \quad (8)$$

$$\tau_2=\frac{n_a(2\pi mk_BT_i)^{1/2}}{P_0S\ \exp(-\delta E_a/k_BT_i)} \quad (9)$$

as the adsorption time and the time of full coverage of the adlayer, respectively.

III. RESULTS AND DISCUSSION

The calculations have been performed for the specific case of the kinetically controlled physical vapor transport growth of α-HgI_2 crystals, which takes place during the initial stage of the process. The consideration is focused only on the $\{110\}$ facet with the sequence of steps growing in directions $\langle001\rangle$ and $\langle1\bar{1}0\rangle$. The energy of adsorption on the $\{110\}$ face is considered to be within $E_a=\Delta H/2-2\Delta H/3$ (where $\Delta H=1.833\times10^{-19}$ J=1.15 eV is the energy of sublimation per one molecule).[24] The activation energy of the surface diffusion is taken as $E_d=0.2E_a$ ($E_d=0.2-0.5E_a$).[9] The activation energy of the molecule incorporation into the steps has been varied within $\delta E_{\rm inc}=0.2-0.5$ eV. The density of adsorption sites on the $\{110\}$ face is estimated as $n_a=2/\sqrt{2}ac\approx2.6\times10^{18}$ m^{-2}, where $a=4.35\times10^{-10}$ m and $c=12.34\times10^{-10}$ m are the unit cell dimensions. The intermolecular distance at the step is $a_0=a=4.35\times10^{-10}$ m and $a_0=a=6.16\times10^{-10}$ m, respectively, for the $\{001\}$ and $\{1\bar{1}0\}$ faces. The height of the monolayer in the $\langle110\rangle$ direction is $h=a/\sqrt{2}\cong3.1\times10^{-10}$ m. The mean distance between the kinks at the steps has been varied within $\lambda_k=1-4a_0$. The characteristic area per molecule in the (110) layer is $s_0=\sqrt{2}ac/2\cong3.7\times10^{-19}$ m^2. To be more specific, operational parameters corresponding to an actual growth experiment[14] with the interstep width within $\lambda=30-50$ μm and step height within $H=25-50h$ are used. The temperatures at the crystal holder and at the source are taken as $T_{\rm sub}=378$ K and $T_0=383$ K, respectively. We neglect here the heat resistance of the crystal, assuming $T_i=T_{\rm sub}$ corresponding to the initial stage of growth. The corresponding growth rate observed was $R\cong7\times10^{-8}$ m/s.

In Figs. 1(a)–1(c) we present the value of the maximal coverage factor on the terrace n/n_a (at a distance from the step much larger than the diffusion length), growth rate

$$R\cong\frac{VH}{\lambda}, \quad (10)$$

and characteristic time τ^*, correspondingly. Graphs are given for different values of energy of adsorption varied within $E_a=\Delta H/2-2\Delta H/3$ in dependence on the value of the steric factor. The calculations are performed for the case of $\lambda=30$ μm and for surface diffusion controlled mode of step-flow growth ($\delta E_{\rm inc}=0$ and $D/\beta\lambda_D\ll1$).

Let us consider the value of the maximal coverage factor shown in Fig. 1(a). It is worth noting that its value does not

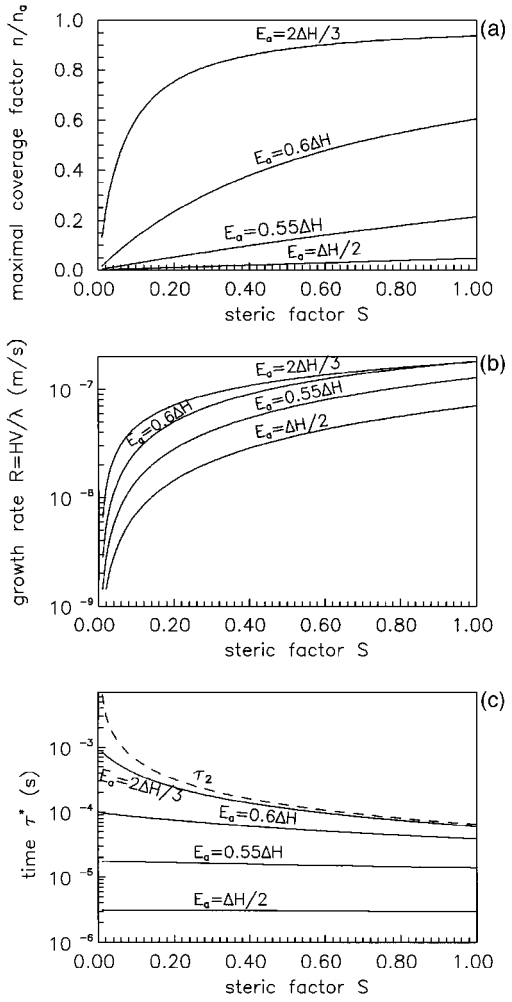

FIG. 1. The dependence of the maximal coverage factor on the terrace (a), growth rate of {110} face (b), and characteristic time of the step-flow model (c) versus the value of steric factor plotted for various values of energy of adsorption.

depend on the activation energy of adsorption.[26] The value of $E_a=2\Delta H/3$ gives very high coverage factor (0.5–0.95) for the range of $S=0.05-1$. Step-flow growth may not be stable with these coverage factors due to the nucleation and growth of two-dimensional islands on the terraces. Lower steric factors, $S<0.05$, giving reasonable values of the coverage factors (<0.3) for $E_a=2\Delta H/3$ lead to growth rates $R<10^{-8}$ m/s which disagree by an order of magnitude with the experimentally observed value of $R=7\times10^{-8}$ m/s. This shows that the value of $E_a=2\Delta H/3$ may not be acceptable for the energy of adsorption on the {110} face. Another limit of $E_a=\Delta H/2$ yields reasonably low coverage factor, even for $S=1$ [Fig. 1(a)]. The relevant growth rate $R\cong7\times10^{-8}$ m/s [Fig. 1(b)] matches well with the experimentally observed value. However, it should be noted that this is a maximal estimate obtained for the minimal value of terrace width $\lambda=30$ μm. Estimate with a larger value of $\lambda=50$ μm gives $R\cong4.2\times10^{-8}$ m/s which does not match its experimental value.

A reasonable range for the activation energy is given by $E_a=(0.55-0.6)\Delta H=0.63-0.69$ eV giving, first, the reasonable values of the coverage factors and, second, growth rates which match well with the experimental values in all ranges of terrace widths and operational conditions. For the case of $E_a=0.6\Delta H=0.69$ eV values of the steric factor within the range $S=0.2-0.4$ [Fig. 1(a)] give a reasonably low maximal coverage factor, within the range of 0.2–0.4, giving good agreement between the relevant growth rates $R=(5-9)\times10^{-8}$ m/s and those of experiments. For the case of $E_a=0.55\Delta H=0.63$ eV the value of the steric factor $S=1$ [Fig. 1(a)] gives reasonably low maximal coverage factors of $\cong0.2$, providing growth rates up to $R=12\times10^{-8}$ m/s. Both these cases exhibit marked inhibition of step-flow velocity (and growth rate) by adsorption and coverage factor n/n_a which inhibits the number of free adsorption sites. That is, for the first case ($E_a=0.6\Delta H=0.69$ eV and $S=0.2-0.4$) the value of the adsorption time [Eq. (8)] $\tau_1\cong10^{-4}$ s while the value of full coverage $\tau_2\cong(2-3)\times10^{-4}$ s [see Fig. 1(c)] so that the characteristic time is in the range of $\tau^*\cong(0.65-0.75)\times10^{-4}$ s. For the second case ($E_a=0.55\Delta H=0.63$ eV and $S=1$) the value of the adsorption time [Eq. (8)] $\tau_1\cong2\times10^{-5}$ s while the value of full coverage $\tau_2\cong7\times10^{-5}$ s [see Fig. 1(c)] so that the characteristic time is $\tau^*\cong1.5\times10^{-5}$ s. The value of the diffusion length $\lambda_D=(D\tau^*)^{1/2}$ is $\lambda_D\cong2.0$ and 1.0 μm, respectively, for the two cases $E_a=0.6\Delta H$, $S=0.2-0.4$ and $E_a=0.55\Delta H$, $S=1$.

In the above calculations the activation energy of adsorbtion was neglected by assuming $\delta E_a=0$. To explore the possible contribution of its effect in Figs. 2(a)–2(c) the dependences of the characteristic time τ^* (a), diffusion length λ_D (b), and growth rate R (c) are given versus the value of δE_a within the range of 0–0.2 eV. Figure 1(a) shows that the value of $\delta E_a=0.1$ eV increases τ^* by an order of magnitude, λ_D by a factor of $\cong\sqrt{10}$, and decreases the growth rate to values $R\cong(1.5-3)\times10^{-8}$ m/s, which do not agree with experimental data. It is reasonable to assume that for relevant coverage factor (with maximal value in the range of 0.2–0.3) molecules impinging into the free adsorbtion sites on the terraces do not overcome any marked energy barrier. In addition, it is worth noting that the coverage factor within one diffusion length (see Fig. 3) from the steps (where the admolecule concentration may be influenced by the value of δE_a) is considerably smaller than that in the middle part of terraces (where the admolecule concentration is not influenced by the value of δE_a).[26]

The typical distributions of the coverage factor n/n_a near the steps for the case with $E_a=0.55\Delta H$ and $S=1$ are shown in Fig. 3 ($\delta E_a=0$) for the two growth directions $\langle001\rangle$ and $\langle110\rangle$ and for various values of the activation energy of incorporation $\delta E_{\rm inc}$. These plots show that the region of nonuniform molecular coverage is located in the vicinity of the steps at a distance of $\cong3$ μm, so that the neighboring steps do not have any diffusion interference with each other. The cases of $\delta E_{\rm inc}=0.4$ and 0.35 eV (curve sets 1 and 2) show a marked difference in n/n_a for the two growth directions, while for the case of $\delta E_{\rm inc}=0.3$ eV (curve set 3) this difference becomes negligibly small. The behavior of the difference of molecular density distributions in front of the step with an increase of $\delta E_{\rm inc}$ may be easily explained in

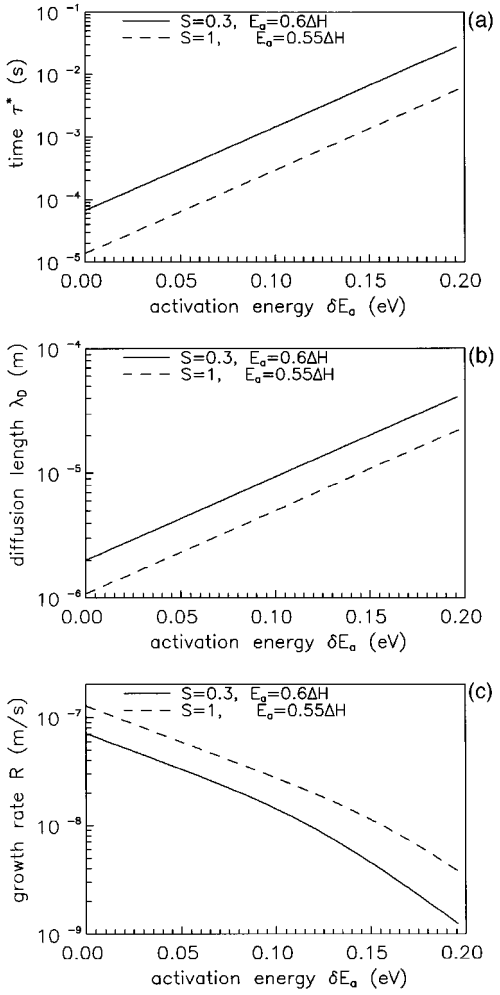

FIG. 2. The dependence of the characteristic time of the step-flow model (a), corresponding diffusion length (b), and growth rate of {110} face (c) versus the value of activation energy of adsorption.

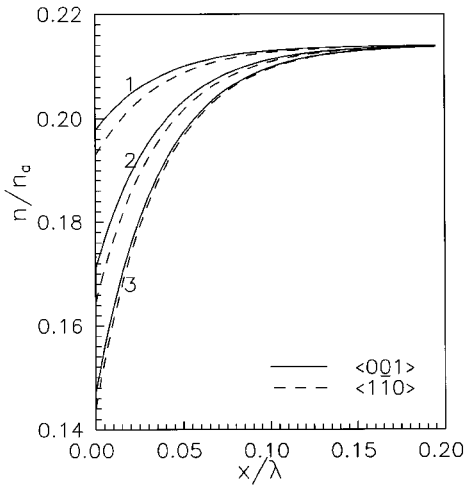

FIG. 3. The distributions of the dimensionless molecular density (coverage factor) in front of the step for two growth directions, $\langle 001\rangle$ and $\langle 1\bar{1}0\rangle$, and different values of activation energy of incorporation: (1) $\delta E_{\rm inc}=0.4$ eV, (2) $\delta E_{\rm inc}=0.35$ eV, (3) $\delta E_{\rm inc}=0.3$ eV.

terms of the kinetic and diffusion resistance of the step-flow growth. For case 1 ($\delta E_{\rm inc}=0.4$ eV), the ratio of the kinetic resistance, $1/\beta$, to the diffusion resistance, λ_D/D, is $[D/\beta\lambda_D]_{\langle 001\rangle}\cong 4.5$ and $[D/\beta\lambda_D]_{\langle 1\bar{1}0\rangle}\cong 3.1$. This results in step-flow velocities in both directions that depend strongly on the corresponding kinetic coefficients $\beta_{\langle 001\rangle}$ and $\beta_{\langle 1\bar{1}0\rangle}$ differing by a factor 1.4 due to the different mean intermolecular distances on the faces. For case 2 ($\delta E_{\rm inc}=0.35$ eV), the values of the ratio $[D/\beta\lambda_D]_{\langle 001\rangle}\cong 1$ and $[D/\beta\lambda_D]_{\langle 1\bar{1}0\rangle}\cong 0.6$. The different step-flow velocities also give different diffusion fluxes at the differently oriented steps, leading to the differences in n/n_a distributions. Therefore, for these two cases, kinetic control is equal to diffusion control by an order of magnitude leading to the marked difference in n/n_a. For case 3, the value of the ratio $[D/\beta\lambda_D]_{\langle 001\rangle}\cong 0.2$ and $[D/\beta\lambda_D]_{\langle 1\bar{1}0\rangle}\cong 0.15$, both being $\ll 1$. This leads to diffusion control of step-flow growth, where the velocity does not depend on the kinetic coefficient and the difference in n/n_a in front of differently oriented steps tends to zero.

To illustrate this Fig. 4(a) presents the dependencies of the step-flow velocities in the two growth directions. Figure 4(b) shows their ratio. In Fig. 4(c), the ratio of kinetic and diffusion resistances, $D/\beta\lambda_D$, is plotted versus the activation energy of incorporation in the range $\delta E_{\rm inc}=0.2-0.5$ eV. The value of $\delta E_{\rm inc}=0.5$ eV corresponds to kinetic control of step-flow growth, the relevant values of $D/\beta\lambda_D\gg 1$ and the step-flow velocities differ as $V_{\langle 1\bar{1}0\rangle}/V_{\langle 001\rangle}\cong 1.4$, in accordance with the difference of the corresponding kinetic coefficients: $\beta_{\langle 1\bar{1}0\rangle}/\beta_{\langle 001\rangle}\cong 1.4$. The values of $\delta E_{\rm inc}<0.3$ eV correspond to diffusion control of step-flow growth, with the relevant values of $D/\beta\lambda_D\ll 1$, causing the step-flow velocities to be the same in both directions $V_{\langle 1\bar{1}0\rangle}/V_{\langle 001\rangle}\cong 1$, since they do not depend on the kinetic coefficients.

Let us discuss how kinetic, diffusion, and kinetic/diffusion growth modes may reveal themselves experimentally. First, under the kinetic regime of step-flow growth, the difference of kinetic coefficients in two perpendicular crystallographic directions on the face should lead to a rectangular form of dislocation spirals with the ratio of lengths of the rectangular sides corresponding to the ratio of the kinetic coefficients in the respective directions. In addition the difference of the kinetic coefficients lead to the difference of the molecular density concentrations near the steps (see Fig. 1). These distributions should overlap near the corners of rectangular spirals leading to a continuous molecular distribution near the corners (since the molecular density distribution is governed by the second-order equation ensuring the distribution continuity). This leads to the corner rounding on the length scale of the diffusion length $\lambda_D\cong 3$ μm. Second, under diffusion control, the step-flow velocity does not depend on the kinetic coefficient and, hence, on the crystallographic direction. Growth of a dislocation spiral with the same velocity in all directions over the face should lead to the rounding and, ideally, to a circular form of dislocation spirals. In addition, under diffusion control, the steps are prone to morphological instabilities leading to their meandering. Finally, the kinetic/diffusion mode of dislocation growth should keep

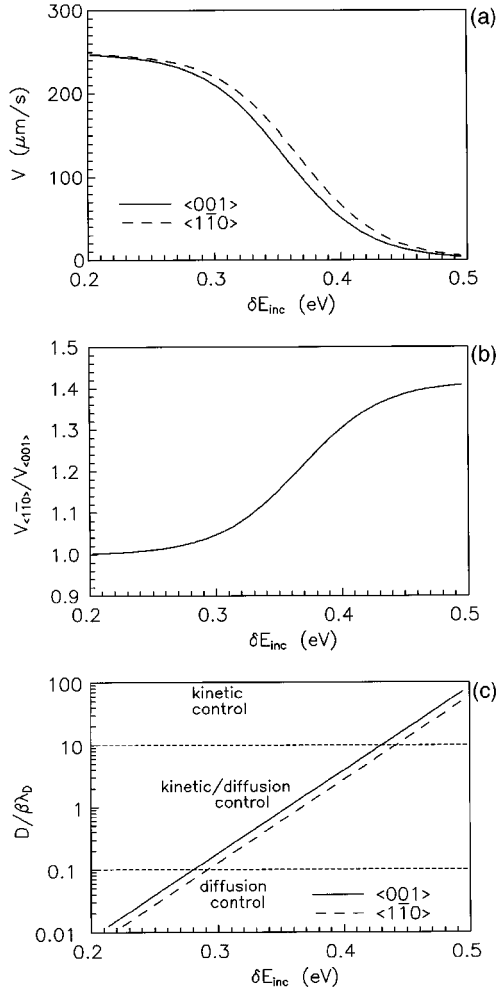

FIG. 4. The dependencies of the step-flow velocity in directions $\langle 001\rangle$ and $\langle 1\bar{1}0\rangle$ (a), their ratio (b) exhibit the equalization of growth velocities in different crystallographic directions along with the decrease of the activation energy of incorporation $\delta E_{\rm inc}$. The ratio of kinetic resistance to diffusion resistance, $D/\beta\lambda_D$, for growth in directions $\langle 001\rangle$ and $\langle 1\bar{1}0\rangle$ (c) exhibits the transition from kinetic to diffusion control along with a decrease in the activation energy of incorporation, $\delta E_{\rm inc}$.

the features of both previously discussed modes. That is, the dislocation spiral should have a rectangular form with rounded sides and corners. Thus, the set of parameters corresponding to the kinetic/diffusion mode with $[D/\beta\lambda_D]_{\langle 001\rangle}\cong 1$, $[D/\beta\lambda_D]_{\langle 1\bar{1}0\rangle}\cong 0.6$, and $V_{\langle 1\bar{1}0\rangle}/V_{\langle 001\rangle}\cong 1.2$ should reveal themselves in dislocation spirals of rectangular form with rounded sides and corners, while the set of parameters corresponding to diffusion control ($D/\beta\lambda_D \ll 1$) should reveal themselves in a circular form of dislocation spirals.

In Figs. 5(a) and 5(b) the values of the step-flow velocity and growth rate are given versus the operational temperature difference between the source and the growth zone for different growth directions and various values of $\delta E_{\rm inc}$ ($E_a=0.55\Delta H$, $S=1$). The step-flow velocity calculated in the framework of the present model for $\delta E_{\rm inc}=0.35$ eV and $\Delta T=5$ K yields a growth rate $R\cong 7-8\times 10^{-8}$ m/s, which agrees well with the growth rates of $R=7\times 10^{-8}$ m/s observed experimentally at the initial stage of growth,[16] when

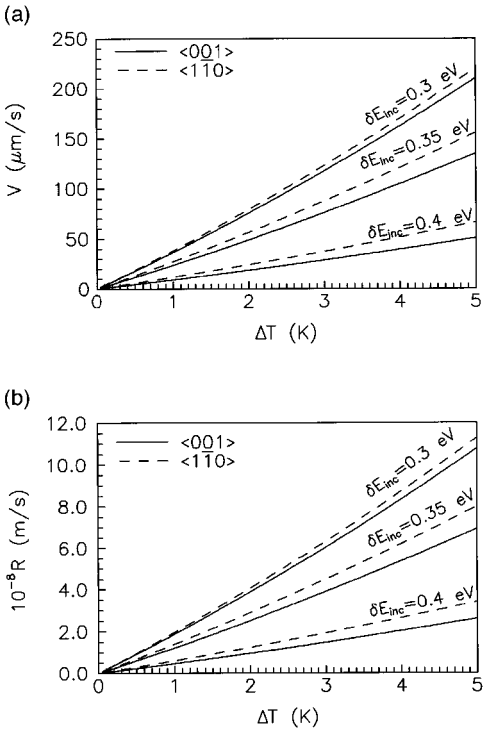

FIG. 5. Step-flow velocity V (a) and corresponding growth rate R (b) plotted for different growth directions and various values of activation energy of incorporation exhibit quasilinear dependence on the operational temperature difference between source and cooled pedestal $\Delta T=T_s-T_{\rm sub}$.

the effects of heat and mass transfer inhibition may be neglected. An estimate of the step-flow velocity for the operational conditions $T_s=388$ K and $T_{\rm sub}=387.4$ K ($\Delta T=0.6$) gives a growth rate of $R=1.25-1.4\times 10^{-8}$ m/s, which matches quite well with the experimental growth rate $R\cong 1.0-1.2\times 10^{-8}$ m/s observed on the initial step in the lateral direction corresponding to the $\{110\}$ face in two sets of growth experiment.[19,20] Moreover, the step-flow velocity V [Fig. 5(a)], and growth rate R [Fig. 5(b)] calculated versus the operational temperature difference between the source and growth pedestal, $\Delta T=T_s-T_{\rm sub}$, exhibit quasilinear dependence over the entire range of $\Delta T=0-5$ K. This explains why linear approximation of the growth rate,[23] $R\propto\beta[P_0-P_{\rm eq}(T_i)]$, with β estimated from one experiment,[14] matches well with experimental data over the entire range of the temperature difference,[14,19] while parabolic approximation[23] of the growth rate estimated from one set of experiments (with $\Delta T=0.6$ K)[19] does not agree with the data of a different experiment (with $\Delta T=5$ K).[14]

IV. CONCLUSIONS

The analysis performed for the step-flow model suggests the following conclusions: (i) Step-flow growth is strongly inhibited by adsorption and high coverage factor ranging from 0.2 to 0.3 and proceeds under kinetic/diffusion or diffusion control, (ii) the time for full coverage of an adlayer is the same order of magnitude as the adsorption time, (iii) the case of kinetic/diffusion control should reveal itself in the rectangular form of dislocation spirals with rounded sides

and corners (the extent of corner rounding should correspond to characteristic diffusion length, $\cong 3$ μm), (iv) the case of diffusion control should reveal itself in the circular form of dislocation spirals, (v) the step-flow velocity and growth rate of {110} face exhibit quasilinear dependence on the operational temperature difference between the source and growth interface in the range of $\Delta T = 0 - 5$ K.

ACKNOWLEDGMENTS

The author would like to express his gratitude to Dr. J. Hester and Dr. A. Matveev of the National Institute for Research in Inorganic Materials (NIRIM) for useful discussions of the problem and to Dr. P. Dennig (NIRIM) for reading the manuscript and providing valuable suggestions.

*Present address: NIRIM 1-1 Namiki, Tsukuba, Ibaraki 305, Japan. Electronic address: loutchev@nirim.go.jp

[1] W. K. Burton, N. Cabrera, and F. C. Frank, Philos. Trans. R. Soc. London Ser. A **243**, 299 (1951).

[2] P. Bennema, J. Cryst. Growth **69**, 182 (1984), and references therein.

[3] A. A. Chernov, *Modern Crystallography III* (Springer-Verlag, Berlin, 1984), and references therein.

[4] G. S. Bales and A. Zangwill, Phys. Rev. B **41**, 5500 (1990).

[5] R. L. Schwoebel, J. Appl. Phys. **40**, 614 (1969).

[6] I. Bena, C. Misbach, and A. Valance, Phys. Rev. B **47**, 7408 (1993).

[7] C. Misbah and W. J. Rappel, Phys. Rev. B **48**, 12 193 (1993).

[8] Y. Saito and M. Uwaha, Phys. Rev. B **49**, 10 677 (1994).

[9] F. Liu and H. Metiu, Phys. Rev. E **49**, 2601 (1994).

[10] A. Pimpinelli, I. Elkinani, A. Karma, C. Misbah, and J. Villain, J. Phys. Condens. Matter **6**, 2661 (1994).

[11] H. A. Lamonds, Nucl. Instrum. Methods **231**, 5 (1983).

[12] E. Kaldis, R. Cadoret, and E. Shonherr, in *Fluid Sciences and Materials Science in Space*, edited by R. V. Walter (Springer-Verlag, Berlin, 1987), pp. 355–404, and references therein.

[13] J. Omali, M. Robert, and R. Cadoret, Mater. Res. Bull. **18**, 785 (1981).

[14] T. Kobayashi, J. T. Muheim, P. Waegly, and E. Kaldis, J. Electrochem. Soc. **130**, 1183 (1983).

[15] V. M. Zaletin, N. V. Lyakh, and N. V. Ragosina, Cryst. Res. Technol. **20**, 307 (1985).

[16] L. van den Berg and W. F. Schnepple, Nucl. Instrum. Methods Phys. Res. Sect. A **283**, 335 (1989).

[17] M. Isshiki, M. Piechotka, and E. Kaldis, J. Cryst. Growth **102**, 344 (1990).

[18] M. Zha, M. Piechotka, and E. Kaldis, J. Cryst. Growth **115**, 43 (1991).

[19] O. A. Louchev, in *Heat Transfer in Phase Change Processes, Proceedings of Eurotherm Seminar 30* (Université Paris-Sud, Orsay, 1992), pp. 201–204.

[20] A. A. Chernov, E. Kaldis, M. Piechotka, and M. Zha, J. Cryst. Growth **125**, 627 (1992).

[21] A. Roux, A. Fedoseyev, and B. Roux, J. Cryst. Growth **130**, 523 (1993).

[22] O. A. Louchev, J. Cryst. Growth **142**, 124 (1994).

[23] O. A. Louchev and V. M. Zaletin, J. Cryst. Growth **148**, 125 (1995).

[24] M. Piechotka and E. Kaldis, J. Less-Common Metals **115**, 315 (1986).

[25] M. M. Factor and I. Carret, *Growth of Crystals from Vapour* (Chapman and Hall, London, 1974).

[26] This is clear from Eq. (1) if one sets $d^2n/dx^2 = 0$.